Supporting Information

Photomechanochemical control over stereoselectivity in the [2+2] photodimerization of acenaphthylene

Sankarsan Biswas,[†a,b,c] Sayan Banerjee,[†d] Milan A. Shlain,[a,b,c] Andrey A. Bardin,[f,g] Rein V. Ulijn,[a,b,c,e] Brent L. Nannenga,[f,g] Andrew M. Rappe,*[d] Adam B. Braunschweig*[a,b,c,e]

[a] S. Biswas, M. A. Shlain, R. V Ulijn, Prof. A. B. Braunschweig
Advanced Science Research Center at the Graduate Center
The City University of New York
85 St. Nicholas Terrace, New York, S NY 10031, United States
E-mail: abraunschweig@gc.cuny.edu

[b] S. Biswas, M. A. Shlain, Prof. R. V Ulijn, Prof. A. B. Braunschweig
The PhD program in Chemistry
The Graduate Center of the City University of New York
365 5th Ave, New York, NY 10016, USA

[c] S. Biswas, M. A. Shlain, Prof. R. V Ulijn, Prof. A. B. Braunschweig
Department of Chemistry
Hunter College
695 Park Ave, New York, NY 10065, USA

[d] S. Banerjee, Prof. A. M. Rappe
Department of Chemistry
University of Pennsylvania
231 S 34th St, Philadelphia, PA 19104, USA
E-mail: rappe@sas.upenn.edu

[e] Prof. R. V Ulijn, Prof. A. B. Braunschweig
The PhD program in Biochemistry
Graduate Center of the City University of New York
365 5th Ave, New York, NY 10016, United States

[f] A. A. Bardin, Prof. B. L. Nannenga
Chemical Engineering
School for Engineering of Matter, Transport, and Energy, Arizona State University
Tempe, AZ 85287, USA

[g] A. A. Bardin, Prof. B. L. Nannenga
Center for Applied Structural Discovery
The Biodesign Institute, Arizona State University
Tempe, AZ 85287, USA

[†] These authors contributed equally to this paper

Table of Contents

1. General methods

All reagents were purchased from Aldrich or VWR and used without further purification unless otherwise noted. Deuterated solvents were purchased from Cambridge Isotope Laboratories Inc. and used as received. NMR spectra were obtained on a Bruker 300 MHz spectrometer. All chemical shifts were reported in ppm units (δ) using residual solvent as the internal reference. HPLC grade solvents were used for all the photocycloaddition experiments. Photocycloaddition reactions were performed in a PhotoRedOx box purchased from HepatoChem (SKU: HCK1006-01-025) unless otherwise noted. All reactions were irradiated with a blue light (HepatoChem, DX Series light 30 W, λ_{max} = 450 nm).

2. Photocycloaddition of acenaphthylene in a modified ball-mill reactor

To carry out the dimerization of acenaphthylene under photomechanochemical conditions, a ball-mill reactor (SPEXSamplePrep, 8000M) was modified (**Figure S1**) with a blue LED (HepatoChem, DX Series light 30 W, λ_{max} = 450 nm), and the reaction was run in a glass vial (20 mL) with two methacrylate balls (SPEXSamplePrep, 8006A, 9.5 mm diameter, 350 mg) so light could reach the reagents during milling. In addition, we found it is necessary to fluorinate the vial[1] and add silica gel (SILICYCLE, SilicaFlash® GE60, Lot # 240320, 70-230 mesh) to the reaction to prevent the reagents from adhering to the side walls. To fluorinate the vial, 4 ml of PhMe was taken in a separate 20 mL vial. 10 drops of heptadecafluoro-1,1,2,2-tetra(hydrodecyl)trichlorosilane was then added to the PhMe-containing vial. The glass vial of interest (for performing photomechanochemistry) and the vial containing the PhMe solution of silane were then kept on opposite sides of a large (~30-cm diameter) vacuum desiccator and vacuum was applied until the PhMe solution began to boil. The desiccator was then kept under static vacuum for 12 h. After 12 h, the vial was removed and washed with PhMe to wash excess silane on the surface. After fluorinating the vial, acenaphthylene (1.2 g) and silica gel (1.2 g) were added to the vial under inert Ar atmosphere, unless otherwise noted, and milled for 20 h at a frequency of 17.7 Hz. Upon completion of the milling, yields and *anti*:*syn* ratios were determined using ^{1}H NMR spectroscopy by dissolving a portion of crude in $CDCl_3$ followed by filtration to remove silica from the $CDCl_3$ solution.

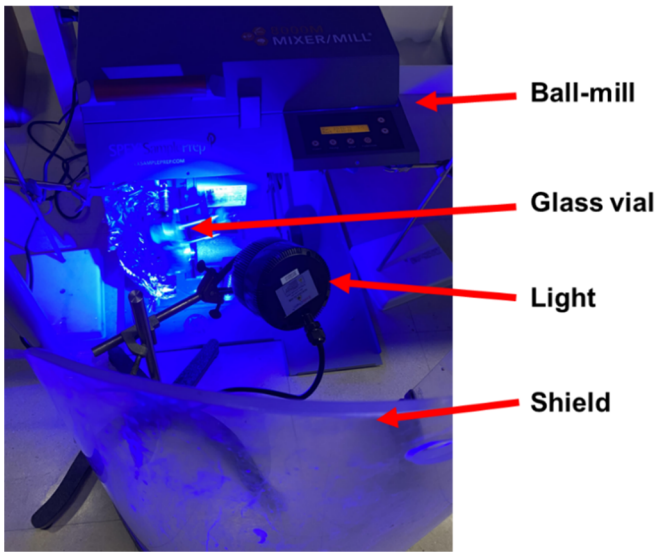

Figure S1. Modified ball-mill for photomechanochemistry

3. Selectivity and Yield calculations from NMR:

For selectivity, integration values for the aliphatic protons **a** and **b** were used (**Figure S2**). It has been reported[2] before that the peak at 4.83 ppm corresponds to the peak **a** from *syn* dimer and the peak at 4.08 ppm corresponds to the **b** from *anti* dimer. So, for the calculation of *anti* selectivity, the formula used was: %anti = **b**/(**a**+**b**)*100. For the yield calculation, disappearance of the peak at 7.07 ppm, which corresponds to peak **c** (**Figure S2**) of the unreacted acenaphthylene was used. So, the formula used for the yield calculation was: yield = (**a**+**b**)/(**a**+**b**+**c**)*100.

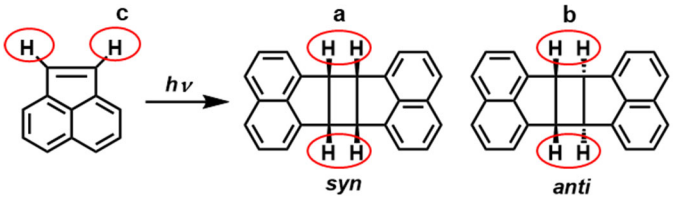

Figure S2. NMR peak assignments for selectivity and yield calculations.

4. NMRs for the photocycloaddition reactions in ball-mill reactor

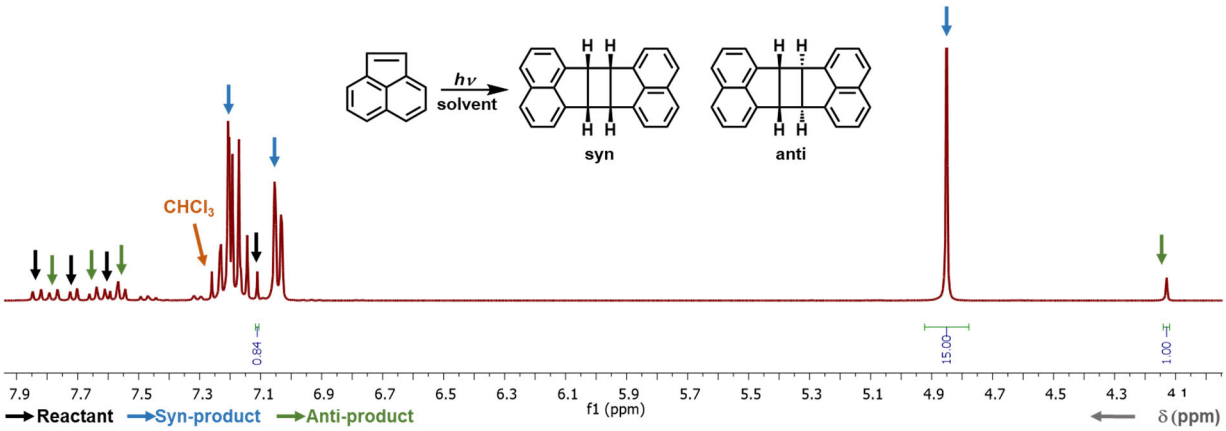

Figure S3. ^{1}H NMR (300 MHz, $CDCl_3$) spectra of the products from photodimerization of acenaphthylene in ball-mill at 25 °C after 20 h of photoirradiation (**Table 1, Entry 1**).

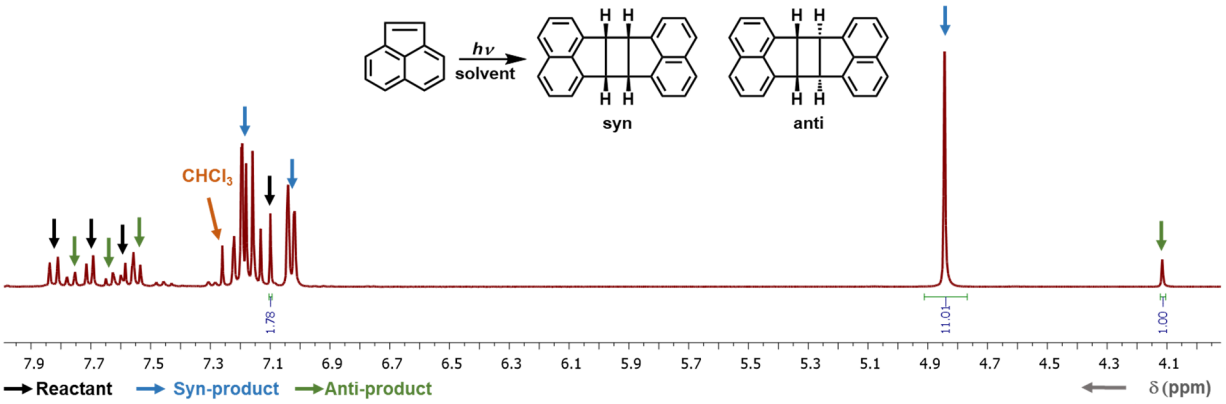

Figure S4. ^{1}H NMR (300 MHz, $CDCl_3$) spectra of the products from photodimerization of acenaphthylene in ball-mill at 25 °C after 20 h of photoirradiation (**Table 1, Entry 2**).

5. Photocycloaddition of acenaphthylene crystals in the absence of ball milling

To determine whether force has a role in stereoselectivity, the reaction was carried out on acenaphthylene crystals by illuminating them in the absence of force. The acenaphthylene crystals (100 mg) were ground with a mortar and pestle, sealed in a petri dish under either inert or ambient atmosphere, and the ground crystals were then irradiated with blue LED (HepatoChem, DX Series light 30 W, λ_{max} = 450 nm) for 20 h (**Table 1, entries 4 – 7**). Upon completion of the reaction, yields and *anti*:*syn* ratios were determined by ^{1}H NMR spectroscopy by dissolving a portion of crude in $CDCl_3$ followed by filtration to remove silica from the $CDCl_3$ solution.

6. NMRs for the photocycloaddition reactions in crystals in the absence of ball milling

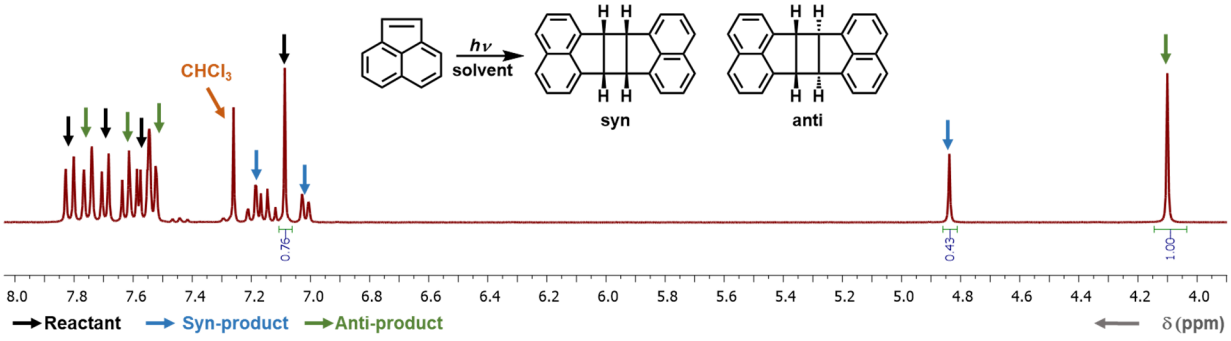

Figure S5. ^{1}H NMR (300 MHz, $CDCl_3$) spectra of the products from photodimerization of acenaphthylene in solid state at 25 °C after 20 h of photoirradiation (**Table 1, Entry 3**).

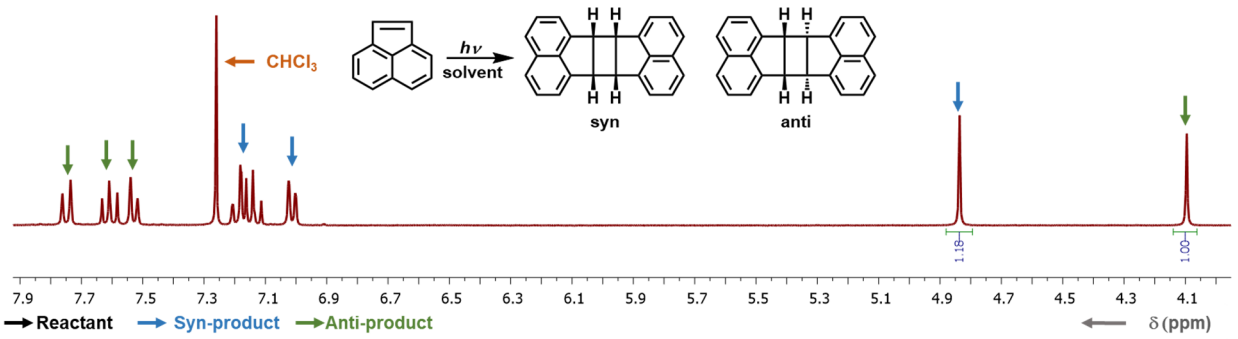

Figure S6. ^{1}H NMR (300 MHz, $CDCl_3$) spectra of the products from photodimerization of acenaphthylene in solid state at 25 °C after 20 h of photoirradiation (**Table 1, Entry 4**).

7. Photocycloaddition of acenaphthylene in solution

To study the effect of solvent on the stereoselectivity of the [2+2] photocycloaddition of acenaphthylene, the reaction was studied in a series of binary solvent mixtures. First, a 5 M solution of acenaphthylene was prepared in DMSO. 4 µL of this stock solution was then added to 1 mL of the desired solvents and sonicated for 1 min to make a homogeneous solution. Ar was bubbled into all solvents for 1 min, before and after the addition of stock solution, to remove dissolved O_2. All reactions were irradiated with a blue light (HepatoChem, DX Series light 30 W, λ_{max} = 450 nm) at room temperature for 2 h, unless otherwise noted. We first tested the photocycloaddition reaction in 6 different solvents, DMSO, EtOH, MeOH, DMF, MeCN, and H_2O. Binary solvent mixtures composed of one organic solvent with varying volume percentages of H_2O were also studied. After each reaction, 1 mL of $CDCl_3$ and 1 mL of H_2O were added directly to the reaction vials to extract the crude products and unreacted acenaphthylene into the organic layer. The organic layer was dried over Na_2SO_4 (anhydrous), and filtered. Selectivities and yields for all reactions were then determined from ^{1}H NMR in $CDCl_3$ (300 MHz) (**Table S1, Figure S9-S24**).

Table S1. Effect of solvent on the [2+2] photocycloaddition of acenaphthylene

Entry	Solvent	Organic Solvent (%)	Yield[d] (%)	*Anti* : *Syn*
8[a]	H_2O	-	84	84:16
9[a]	H_2O / DMSO	25	95	59:41
10[a]	H_2O / DMSO	50	99	31:69
11[a]	DMSO	100	99	49:51
12[a]	H_2O / EtOH	25	72	77:23
13[a]	H_2O / EtOH	50	91	39:61
14[a]	EtOH	100	61	52:48
15[a]	H_2O / MeOH	25	73	78:22
16[a]	H_2O / MeOH	50	92	42:58
17[a]	MeOH	100	64	46:54
18[a]	H_2O / DMF	25	90	47:53
19[a]	H_2O / DMF	50	94	33:67
20[a]	DMF	100	89	47:53
21[a]	H_2O / MeCN	25	83	43:57
22[a]	H_2O / MeCN	50	75	23:77
23[a]	MeCN	100	35	24:76
24[b]	H_2O	-	99	83:17
25[c]	H_2O	-	98	91:9

All reactions contain 0.4 % (v/v) DMSO and 3.0 mg of acenaphthylene in 1 mL solvent. All solvents were purged with Ar. Yields and selectivities were determined from ^{1}H NMR in $CDCl_3$. Photocycloaddition reactions were performed in a PhotoRedOx box (HepatoChem; HCK1006-01-025) with a blue LED light (DX Series light 30 W, λ_{max} = 450 nm). [a] Reactions were stopped after 2 h of photoirradiation at 25 ^{o}C. [b] Reaction was stopped after 16 h of photoirradiation at 25 ^{o}C. [c] Reaction was stopped after 16 h of photoirradiation at 10 ^{o}C. [d] Yield: Combined yields of *syn* and *anti* products.

8. NMRs for the photocycloaddition reactions in solvents

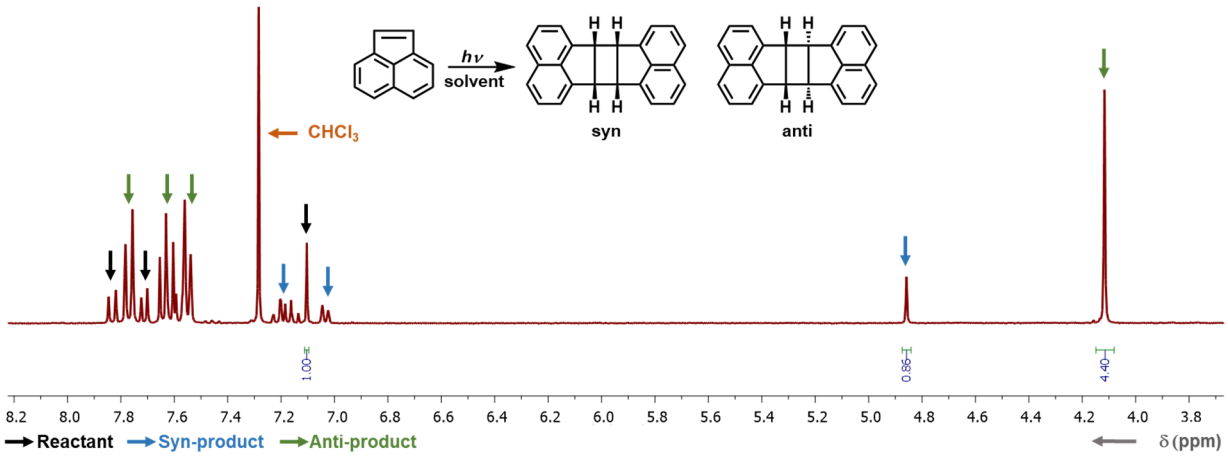

Figure S7. ^{1}H NMR (300 MHz, $CDCl_3$) spectra of the products from photodimerization of acenaphthylene in H_2O at 25 °C after 2 h of photoirradiation (**Table S1, Entry 8**).

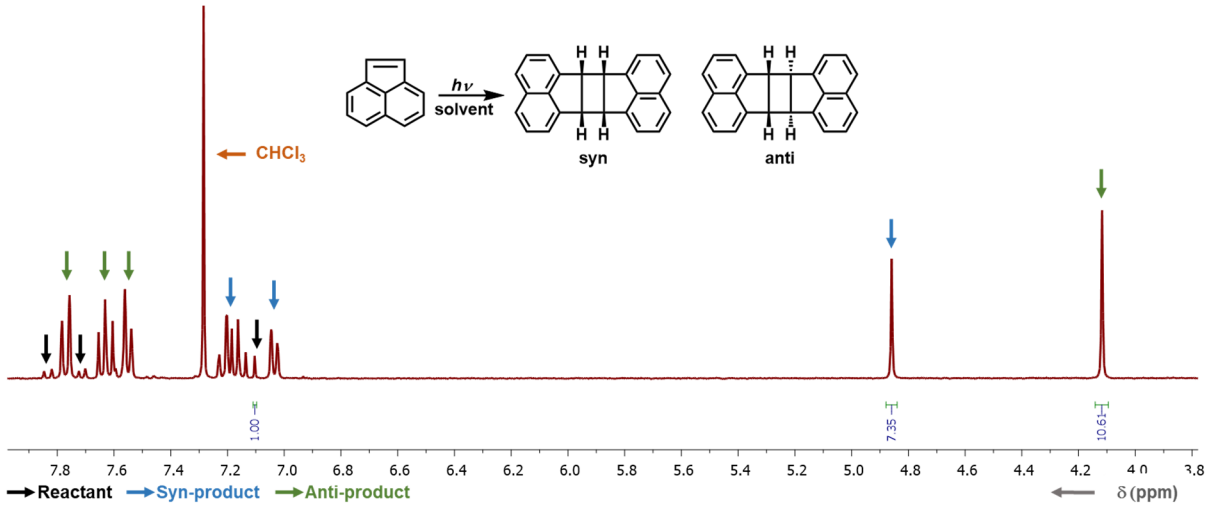

Figure S8. ^{1}H NMR (300 MHz, $CDCl_3$) spectra of the products from photodimerization of acenaphthylene in 25% DMSO (in H_2O) at 25 °C after 2 h of photoirradiation (**Table S1, Entry 9**).

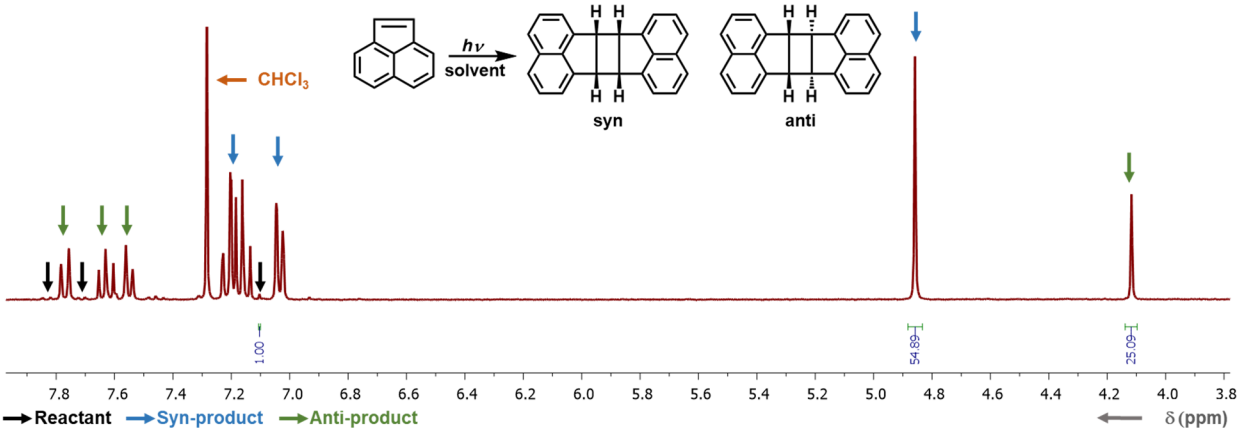

Figure S9. ^{1}H NMR (300 MHz, $CDCl_3$) spectra of the products from photodimerization of acenaphthylene in 50% DMSO (in H_2O) at 25 °C after 2 h of photoirradiation (**Table S1, Entry 10**).

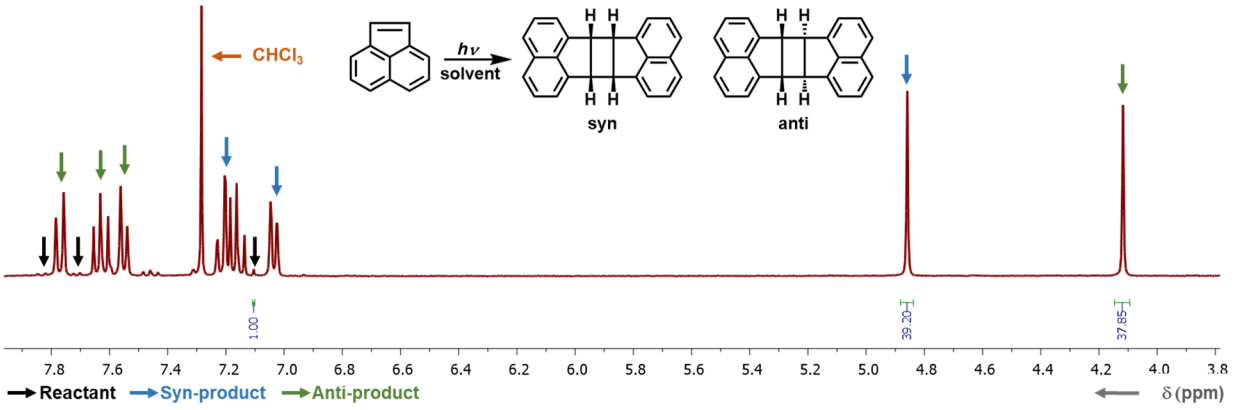

Figure S10. ^{1}H NMR (300 MHz, $CDCl_3$) spectra of the products from photodimerization of acenaphthylene in 100% DMSO at 25 °C after 2 h of photoirradiation (**Table S1, Entry 11**).

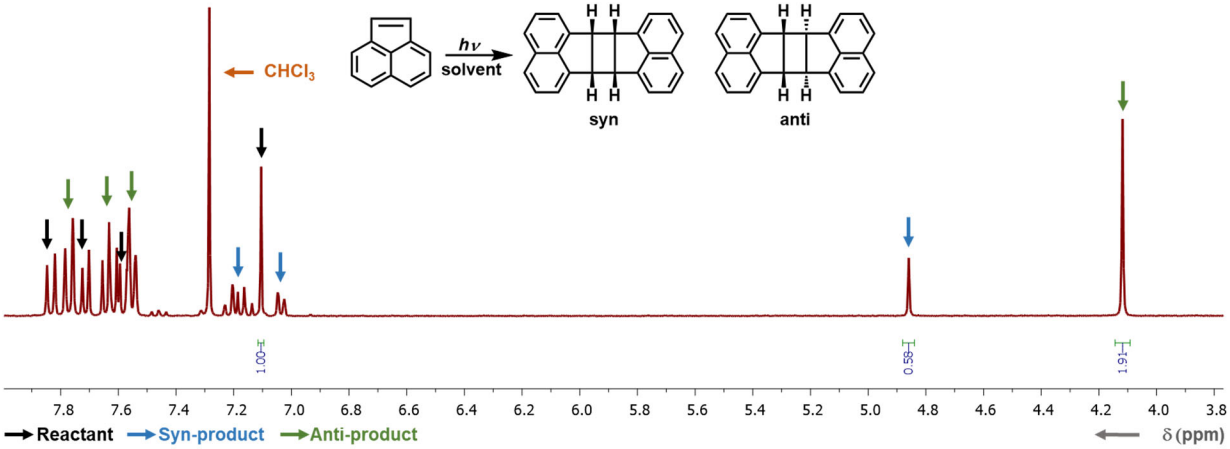

Figure S11. ^{1}H NMR (300 MHz, $CDCl_3$) spectra of the products from photodimerization of acenaphthylene in 25% EtOH (in H_2O) at 25 °C after 2 h of photoirradiation (**Table S1, Entry 12**).

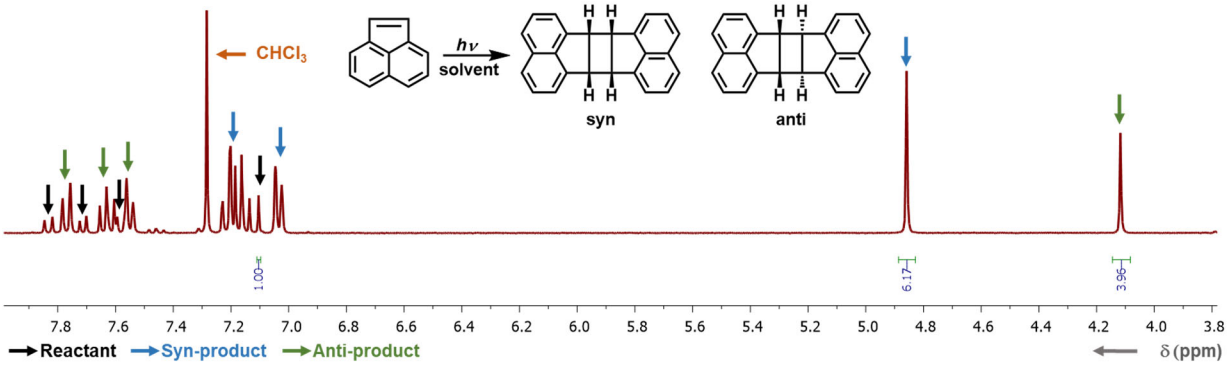

Figure S12. ^{1}H NMR (300 MHz, $CDCl_3$) spectra of the products from photodimerization of acenaphthylene in 50% EtOH (in H_2O) at 25 °C after 2 h of photoirradiation (**Table S1, Entry 13**).

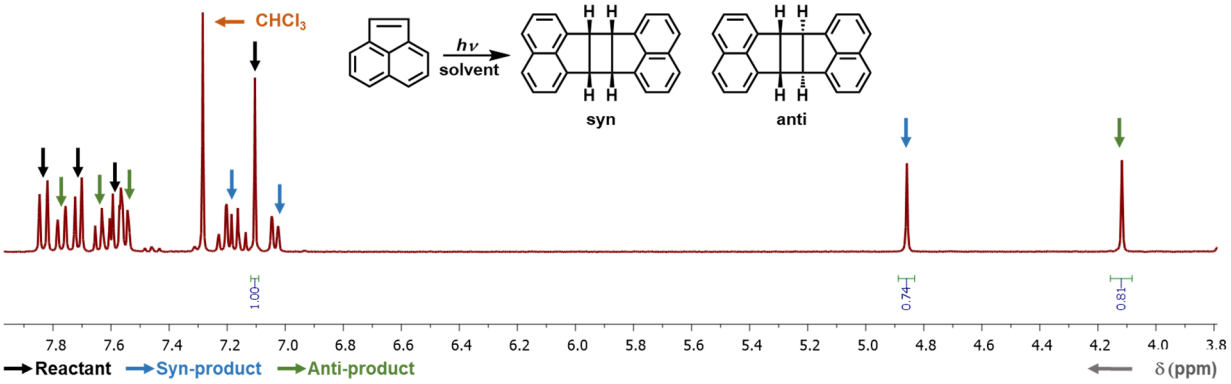

Figure S13. ^{1}H NMR (300 MHz, $CDCl_3$) spectra of the products from photodimerization of acenaphthylene in 100% EtOH at 25 °C after 2 h of photoirradiation (**Table S1, Entry 14**).

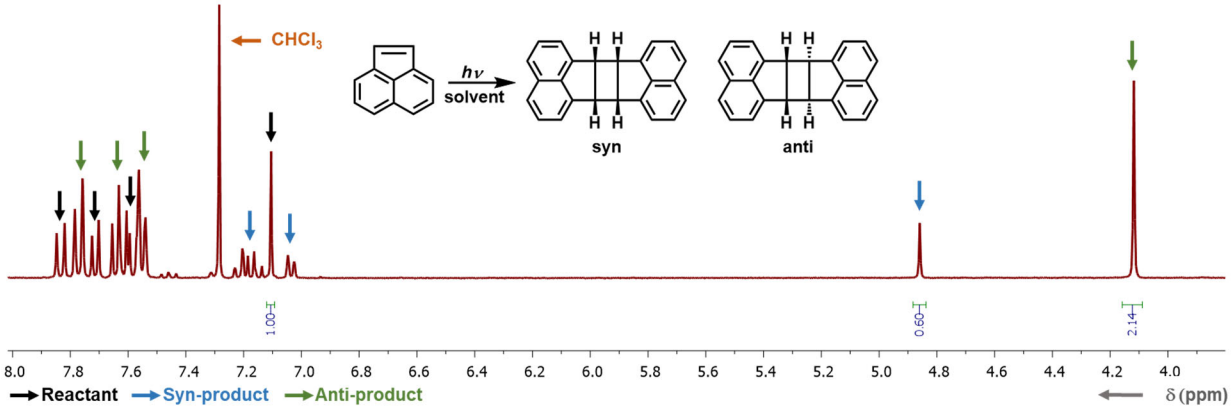

Figure S14. ^{1}H NMR (300 MHz, $CDCl_3$) spectra of the products from photodimerization of acenaphthylene in 25% MeOH (in H_2O) at 25 °C after 2 h of photoirradiation (**Table S1, Entry 15**).

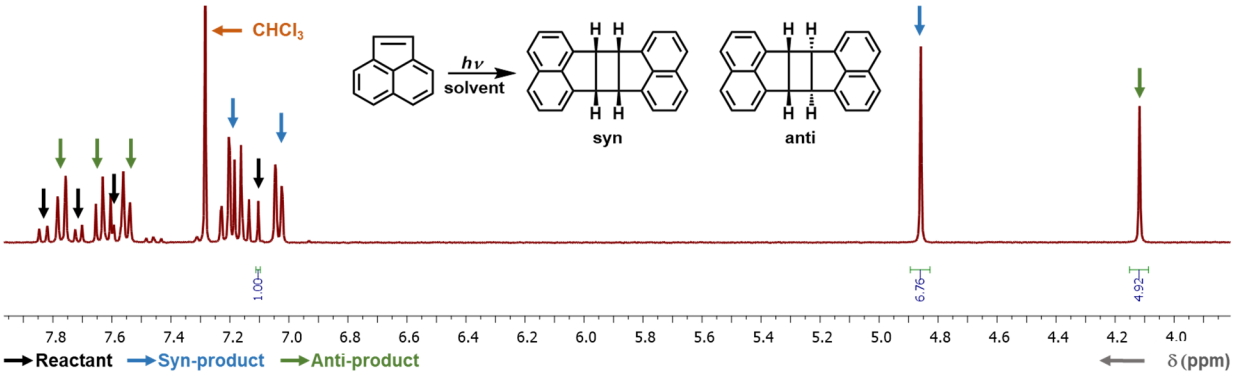

Figure S15. ^{1}H NMR (300 MHz, $CDCl_3$) spectra of the products from photodimerization of acenaphthylene in 50% MeOH (in H_2O) at 25 °C after 2 h of photoirradiation (**Table S1, Entry 16**).

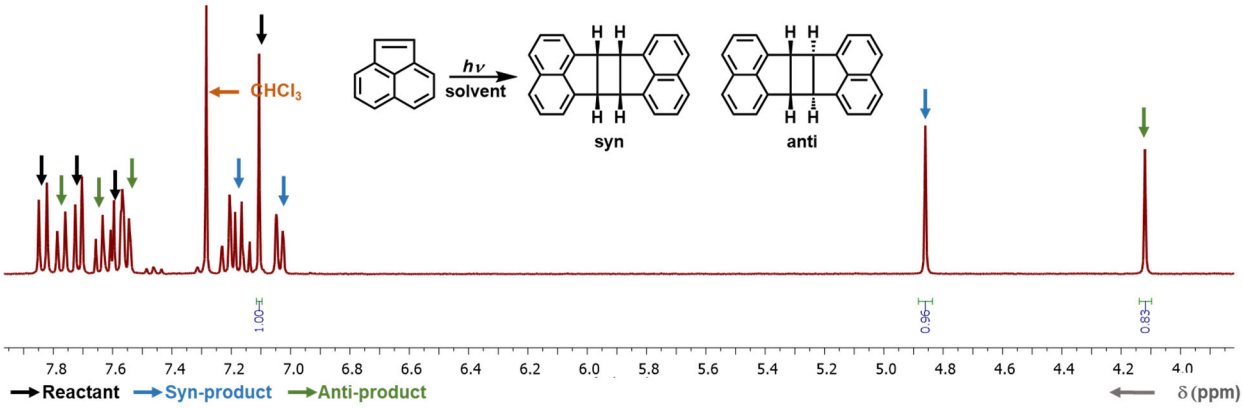

Figure S16. ^{1}H NMR (300 MHz, $CDCl_3$) spectra of the products from photodimerization of acenaphthylene in 100% MeOH at 25 °C after 2 h of photoirradiation (**Table S1, Entry 17**).

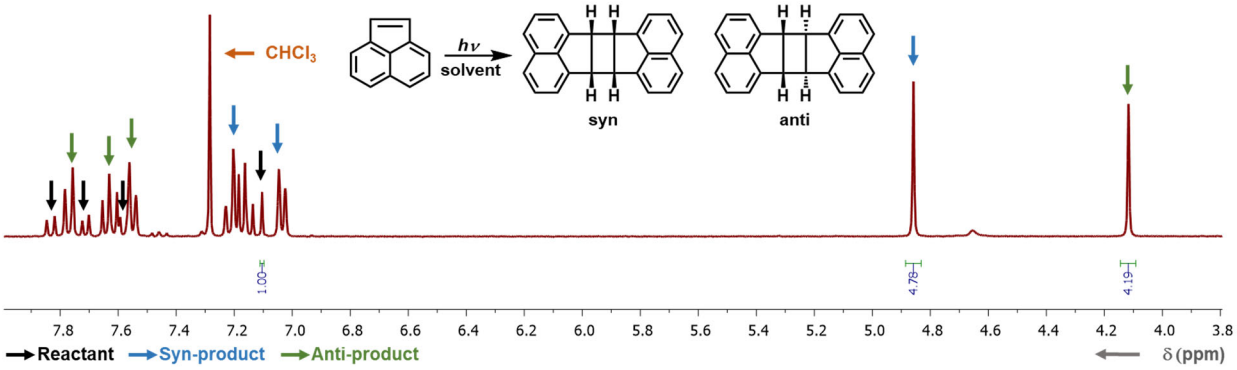

Figure S17. ^{1}H NMR (300 MHz, $CDCl_3$) spectra of the products from photodimerization of acenaphthylene in 25% DMF (in H_2O) at 25 °C after 2 h of photoirradiation (**Table S1, Entry 18**).

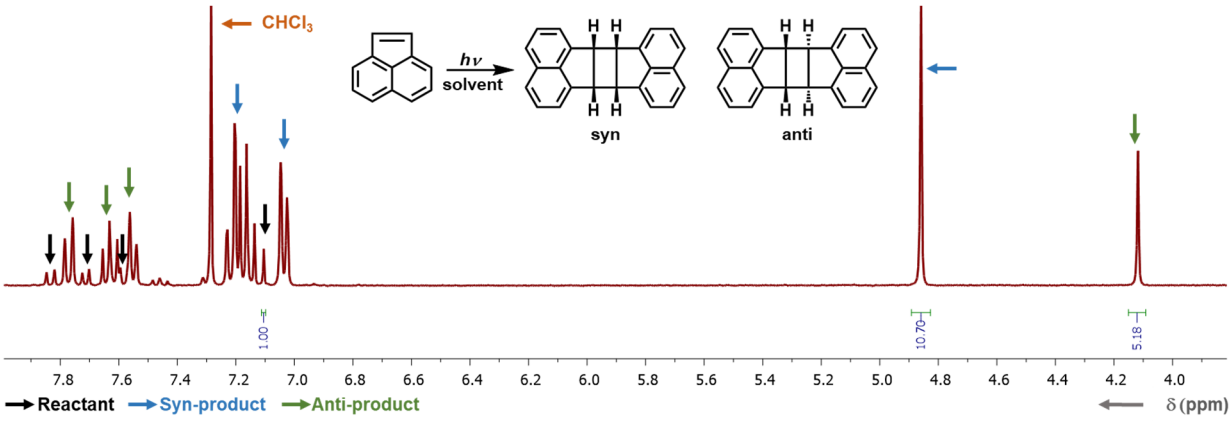

Figure S18. ^{1}H NMR (300 MHz, $CDCl_3$) spectra of the products from photodimerization of acenaphthylene in 50% DMF (in H_2O) at 25 °C after 2 h of photoirradiation (**Table S1, Entry 19**).

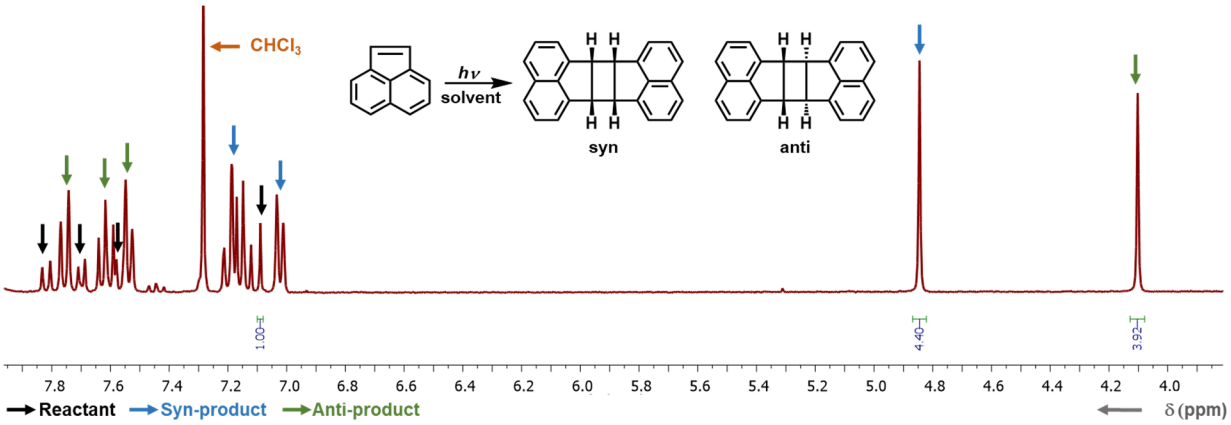

Figure S19. ^{1}H NMR (300 MHz, $CDCl_3$) spectra of the products from photodimerization of acenaphthylene in 100% DMF at 25 °C after 2 h of photoirradiation (**Table S1, Entry 20**).

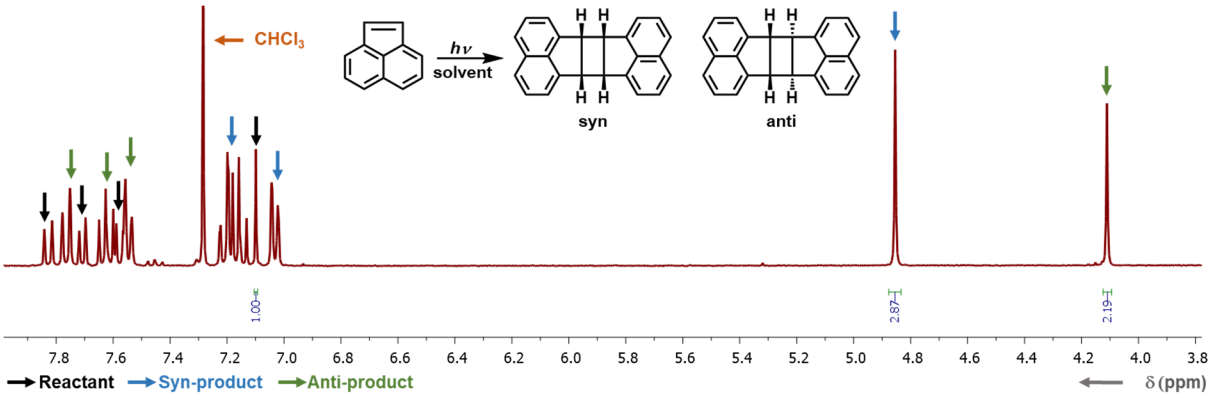

Figure S20. ^{1}H NMR (300 MHz, $CDCl_3$) spectra of the products from photodimerization of acenaphthylene in 25% MeCN (in H_2O) at 25 °C after 2 h of photoirradiation (**Table S1, Entry 21**)

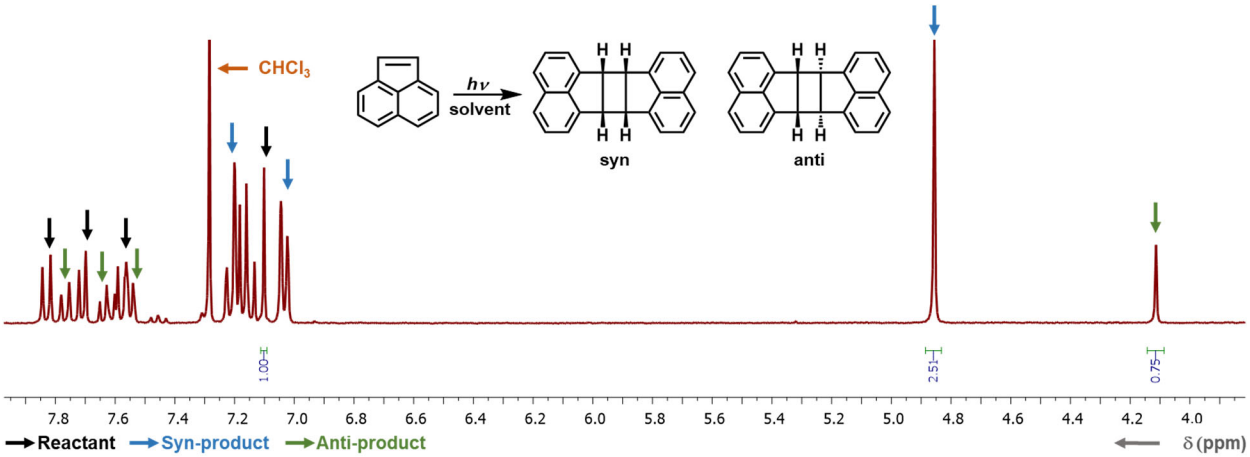

Figure S21. ^{1}H NMR (300 MHz, $CDCl_3$) spectra of the products from photodimerization of acenaphthylene in 50% MeCN (in H_2O) at 25 °C after 2 h of photoirradiation (**Table S1, Entry 22**).

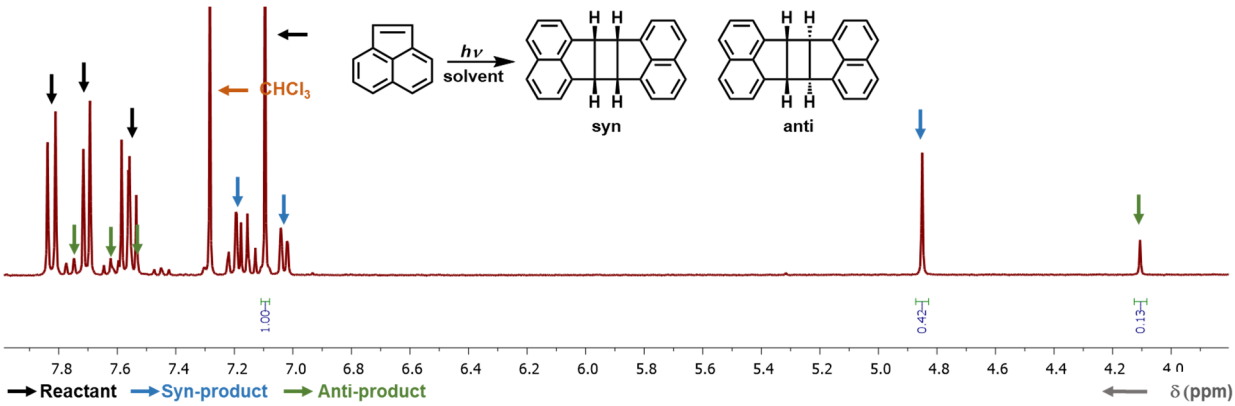

Figure S22. ^{1}H NMR (300 MHz, $CDCl_3$) spectra of the products from photodimerization of acenaphthylene in 100% MeCN at 25 °C after 2 h of photoirradiation (**Table S1, Entry 23**).

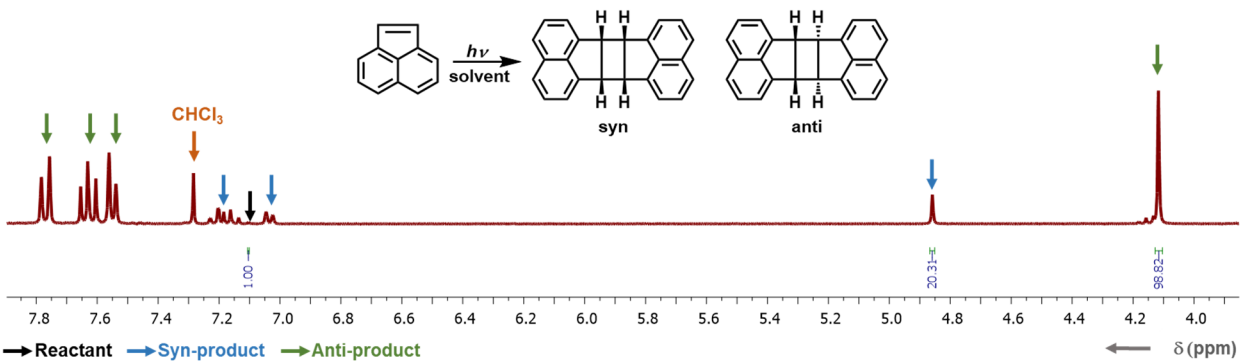

Figure S23. ^{1}H NMR (300 MHz, $CDCl_3$) spectra of the products from photodimerization of acenaphthylene in 100% H_2O at 25 °C after 16 h of photoirradiation (**Table S1, Entry 24**).

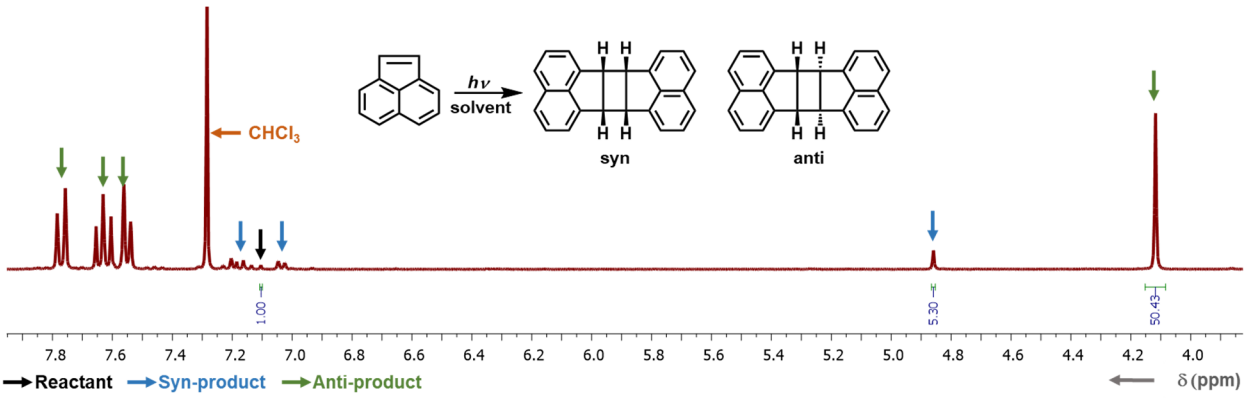

Figure S24. ^{1}H NMR (300 MHz, $CDCl_3$) spectra of the products from photodimerization of acenaphthylene in 100% H_2O at 10 °C after 16 h of photoirradiation (**Table S1, Entry 25**).

9. Microcrysalline Electron Diffraction (MicroED)

Sample Preparation

3-5 µL of 20 mM acenaphthylene solutions in $CHCl_3$ were applied to the surface of continuous carbon coated copper mesh EM grids [Electron Microscope Sciences CF400-CU] for 20 sec and then wicked dry from the grid edge using filter paper [Whatman Cat No 1001-070].

Data Collection

For the collection of diffraction data, standard MicroED data collection procedures were used as described below[3]. Grids containing the crystalline samples were loaded into a Titan Krios cryo-TEM equipped with a CETA D detector for MicroED data collection, and all steps were performed using the "low dose" mode of the cryo-TEM. Low magnification (LM mode, ~600x) was used to initially screen the quality of the grids and identify promising nanocrystals on the grid. Initial diffraction patterns were collected from single crystals by switching the cryo-TEM into diffraction mode and acquiring an initial diffraction pattern. If this initial diffraction pattern showed high quality diffraction, a full MicroED data set was collected from the crystal. MicroED data sets were collected by continuously rotating the crystal in the beam as the CETA D camera continuously acquired diffraction images.

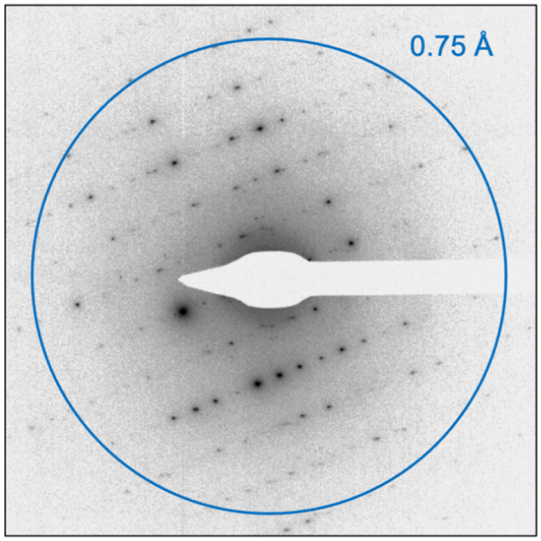

Figure S25. Example diffraction patterns from acenaphthylene crystal MicroED data sets.

Data Processing

MicroED data were converted from MRC to SMV format for further data processing[4]. The data sets were indexed, integrated, and scaled using XDS[5]. Structures were solved by direct methods in SHELXT[6] and refined using SHELXL[7].

CCDC 2167919 contains the supplementary crystallographic data for this paper. These data can be obtained free of charge via www.ccdc.cam.ac.uk/data_request/cif, or by emailing data_request@ccdc.cam.ac.uk, or by contacting The Cambridge Crystallographic Data Centre, 12 Union Road, Cambridge CB2 1EZ, UK; fax: +44 1223 336033.

Table S2. Data collection and refinement statistics.

	acenaphthylene
Data collection	
Excitation Voltage	300 kV
Wavelength (Å)	0.019687
Number of crystals	7
Data Processing[a]	
Space group	$P2_1/n$
Unit cell length a, b, c (Å)	7.72, 4.78, 19.85
Angles α, β, ɣ (°)	90.000, 92.219, 90.000
Resolution (Å)	10.00 - 0.80 (0.83 - 0.80)
Number of reflections	13,453
Unique reflections	1,494
R_{obs} (%)	33.8 (84.8)
R_{meas} (%)	35.8 (107.9)
I/σ_I	3.44 (0.61)
$CC_{1/2}$ (%)	97.2 (50.2)
Completeness (%)	89.4 (55.0)
Structure Refinement	
R1[b]	0.2738 (0.2174)
wR2	0.4720
GooF	1.376

[a] Values in parentheses represent the highest resolution shell

[b] Values in parentheses represent the R1 for $F^2_o > 2\sigma(F^2_o)$

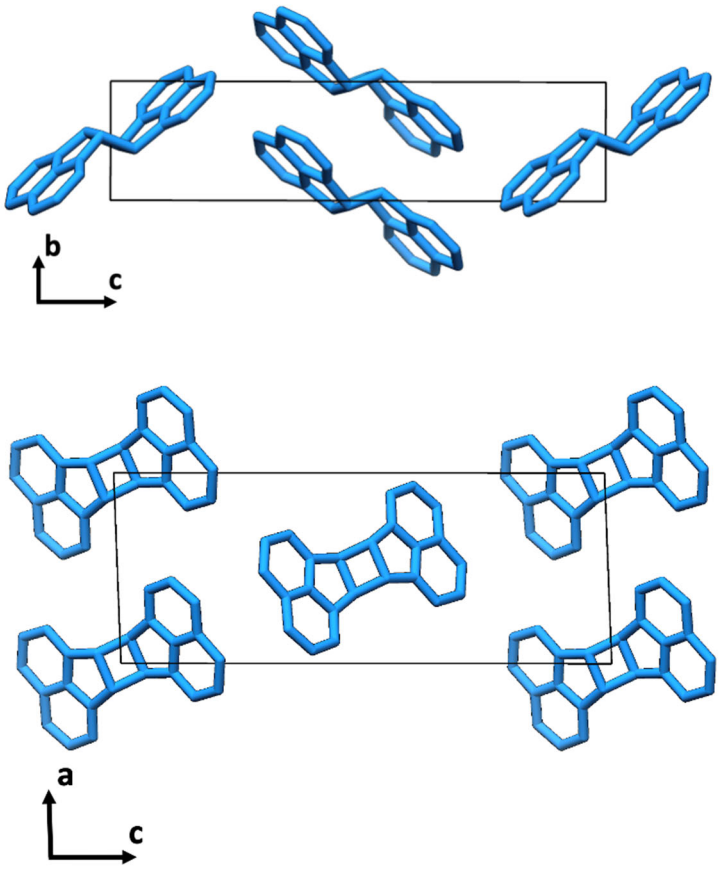

Figure S26. MicroED structure of *anti* dimer of acenaphthylene (CCDC 2167919).

10. Computational Details

The density functional theory (DFT) calculations were performed using B3LYP-D3 hybrid density functional in conjunction with Pople's 6-31G(d) basis set as implemented in Q-Chem quantum chemistry package.[8] The energy difference between the *syn* and *anti* initial state supramolecular conformer dimer was benchmarked using both B3LYP-D3/6-31G(d) and M06-2X-D3/6-31G(d) level of theory. The *syn* conformer supramolecular dimer is found to be stable by 8.99 and 8.91 kJ/mol than the *anti* using B3LYP-D3/6-31G(d) and M06-2X-D3/6-31G(d), respectively, thereby suggesting no significant dependence on the level of theory used between these two. Here, we have used the initial supramolecular states obtained from M06-2X-D3/6-31G(d), as B3LYP-D3/6-31G(d) was unable converge in a geometry similar to the supramolecular dimer. As such, supramolecular dimers (**Figure 2**) are a more reasonable approximation of the initial states in a solid-state crystal. The geometry from M06-2X-D3/6-31G(d) was considered and then a constrained optimization was performed using B3LYP-D3/6-31G(d) to properly scale the energy in **Figure 2**. The force in the simulation was applied by external force explicitly included (EFEI) method.[9] Note that the reported data regarding EFEI was performed using a B3LYP hybrid density functional in conjunction with Pople's 6-31G(d), and dispersion correction was not used as there were convergence issues observed while using EFEI and dispersion correction together. The transition states were

characterized by one and only one imaginary frequency, and the transition states coordinates are given in **Table S2**. The energy decomposition analysis (EDA)[10] was carried out to understand the effect of force on the acenaphthylene *syn* and *anti* supramolecular conformers. In this case, the monomers were considered as separate fragments and the electronic interaction between them was quantified through EDA. Here, a single point calculation was performed on the optimized geometry obtained by EFEI calculations. The total interaction energy is considered as the summation of the frozen density term (E_{FZ}), the polarization term (E_{Pol}), and the charge transfer term (E_{CT}). E_{FZ} is defined as the change in SCF energy which corresponds to bringing infinitely separated distorted molecules into the given geometry without any relaxation of the molecular orbitals (MO), which are localized on each fragment. E_{FZ} consists of both Coulomb and exchange terms between the electron clouds on each fragment and is repulsive when the fragments move close to each other because of higher electrostatic repulsion. E_{Pol} is calculated by allowing the relaxation of the MOs on each fragment under the presence of the field of other fragments. While calculating the E_{Pol}, the MOs are not allowed to mix between fragments. Next, the E_{CT} is calculated by allowing the full relaxation of MOs and therefore charge can flow between the fragments. All the values are calculated using the Q-Chem quantum chemistry package. The reported charge transfer values were calculated using the Roothan step correction. The vertical excitation energies reported in **Figure 2** were calculated using a time dependent DFT calculation with the Tamm-Dancoff approximation at B3LYP-D3/6-31G(d) level of theory.

Table S2. Transition state (TS) coordinates for *syn* and *anti* product formation

TS for *syn*			
C	-0.042559938	1.710588072	-2.192453605
C	-0.52713674	0.409128497	-1.928094481
C	1.25717469	2.097945754	-1.882834486
C	0.33293665	-0.487611166	-1.310053886
C	0.242008099	-1.914187715	-0.962229084
C	2.156127652	1.203173368	-1.241441217
C	1.626038213	-0.058648338	-0.92976237
C	1.473531424	-2.242821092	-0.233785546
C	2.348668887	-1.118581834	-0.300710792
C	3.529562894	1.400253683	-0.917320963
C	3.681317978	-0.880363155	0.024814472
C	4.245068359	0.373705158	-0.313471313
C	-1.438961041	-2.332241105	0.331259621
C	-0.279866807	-2.015032723	1.166303281
C	-2.328629361	-1.206952511	0.326964902
C	-0.421412402	-0.62071592	1.55123739
C	-3.584205375	-0.920750665	-0.210281588
C	-1.664724065	-0.171531107	1.043642649
C	0.405624379	0.278514289	2.203820269
C	-4.135505218	0.369114172	0.00197046
C	-2.174579241	1.12373714	1.224636655
C	-0.067900476	1.596785919	2.380951093
C	-3.471049431	1.37704993	0.687858161

C	-1.316615555	2.01200896	1.925844892
H	-0.705114106	2.426560972	-2.671006266
H	-1.544783437	0.136324964	-2.187915436
H	-0.235248487	-2.61060743	-1.643015305
H	1.774597655	-3.263881925	-0.033184945
H	4.298119087	-1.653859316	0.474415948
H	5.299275797	0.531789694	-0.098942037
H	1.592646653	3.098477093	-2.144683077
H	4.018185189	2.337402889	-1.166863825
H	-1.7148385	-3.344350054	0.060388808
H	0.254549187	-2.747424363	1.754978929
H	-4.154524834	-1.666710535	-0.758008154
H	1.393401545	-0.011766067	2.546239286
H	-5.12714727	0.576423879	-0.393632489
H	0.57034067	2.314261173	2.888963913
H	-3.931414404	2.352567086	0.818175441
H	-1.631302316	3.038439941	2.099085942
TS for *anti*			
H	2.656971994	2.111239724	-3.254064185
H	0.584013589	1.568642691	-2.027593859
C	2.697718402	1.368380917	-2.461643357
C	1.505872988	1.075350637	-1.745360977
H	-0.355123363	-0.900077007	-0.36622987
C	3.896450612	0.725989307	-2.198453409
C	1.54809445	0.141788774	-0.726680995
C	0.503542521	-0.499710434	0.182314691
C	3.96040799	-0.270008228	-1.186075608
C	2.774950426	-0.497156159	-0.470228843
C	1.265679403	-1.497166314	0.929316252
C	2.611642673	-1.524917025	0.514604091
C	5.057097626	-1.127659177	-0.879564025
H	0.829414441	-2.135815862	1.687898736
C	3.71531893	-2.34468296	0.790188048
C	4.913909999	-2.127682969	0.078846672
H	3.645858772	-3.160548934	1.504364255
H	5.757793776	-2.78398411	0.276408089
H	4.780267567	0.959339911	-2.787075217
H	5.991011359	-1.027015497	-1.425837294
H	-0.619859862	-0.72916368	3.007203225
C	-1.117409287	-0.190364036	2.210493713
C	-0.411086259	0.600846328	1.204132163
H	0.365884909	1.284185267	1.546803188
C	-2.483196127	-0.303930712	1.882170697
C	-1.531109254	1.189471448	0.355376892

C	-3.580952677	-1.02368595	2.384856062
C	-2.711804099	0.534567539	0.742980951
C	-1.611293484	2.113035191	-0.670381665
C	-4.83362018	-0.890538165	1.749956879
H	-3.480297529	-1.675418158	3.248177331
C	-3.960544669	0.693882622	0.114908113
C	-2.860196949	2.313888271	-1.322182861
H	-0.749686597	2.689381342	-0.989920119
H	-5.675260021	-1.454487007	2.145066277
C	-5.043327889	-0.062414314	0.649530857
C	-4.002353115	1.615742614	-0.966489301
H	-2.910958645	3.033798016	-2.134880047
H	-6.033858311	0.020916358	0.209640376
H	-4.934999723	1.782984939	-1.500491762

11. References

[1] a) D. Ge, L. Yang, G. Wu, S. Yang, *Chem. Commun.* **2014**, *50*, 2469-2472; b) D. J. Eichelsdoerfer, X. Liao, M. D. Cabezas, W. Morris, B. Radha, K. A. Brown, L. R. Giam, A. B. Braunschweig, C. A. Mirkin, *Nat. Protoc.* **2013**, *8*, 2548-2560.

[2] V. Ramesh, V. Ramamurthy, *J. Photochem.* **1984**, *24*, 395-402.

[3] B. L. Nannenga, T. Gonen, *Nat. Methods* **2019**, *16*, 369-379.

[4] J. Hattne, M. W. Martynowycz, T. Gonen, *bioRxiv* **2019**, 615484.

[5] W. Kabsch, *Acta Crystallogr. D* **2010**, *66*, 125-132.

[6] G. M. Sheldrick, *Acta Crystallogr. A* **2015**, *71*, 3-8.

[7] G. M. Sheldrick, *Acta Crystallogr. C Struct* **2015**, *71*, 3-8.

[8] Y. Shao, L. F. Molnar, Y. Jung, J. Kussmann, C. Ochsenfeld, S. T. Brown, A. T. B. Gilbert, L. V. Slipchenko, S. V. Levchenko, D. P. O'Neill, R. A. DiStasio Jr, R. C. Lochan, T. Wang, G. J. O. Beran, N. A. Besley, J. M. Herbert, C. Yeh Lin, T. Van Voorhis, S. Hung Chien, A. Sodt, R. P. Steele, V. A. Rassolov, P. E. Maslen, P. P. Korambath, R. D. Adamson, B. Austin, J. Baker, E. F. C. Byrd, H. Dachsel, R. J. Doerksen, A. Dreuw, B. D. Dunietz, A. D. Dutoi, T. R. Furlani, S. R. Gwaltney, A. Heyden, S. Hirata, C.-P. Hsu, G. Kedziora, R. Z. Khalliulin, P. Klunzinger, A. M. Lee, M. S. Lee, W. Liang, I. Lotan, N. Nair, B. Peters, E. I. Proynov, P. A. Pieniazek, Y. Min Rhee, J. Ritchie, E. Rosta, C. David Sherrill, A. C. Simmonett, J. E. Subotnik, H. Lee Woodcock Iii, W. Zhang, A. T. Bell, A. K. Chakraborty, D. M. Chipman, F. J. Keil, A. Warshel, W. J. Hehre, H. F. Schaefer Iii, J. Kong, A. I. Krylov, P. M. W. Gill, M. Head-Gordon, *Phys. Chem. Chem. Phys.* **2006**, *8*, 3172-3191.

[9] J. Ribas-Arino, M. Shiga, D. Marx, *Angew. Chem. Int. Ed.* **2009**, *48*, 4190-4193.

[10] R. Z. Khaliullin, E. A. Cobar, R. C. Lochan, A. T. Bell, M. Head-Gordon, *J. Phys. Chem. A* **2007**, *111*, 8753-8765.